Equations of state and transport properties of mixtures in the warm dense regime

Article *in* Physics of Plasmas · February 2015

Impact Factor: 2.14 · DOI: 10.1063/1.4913424

5 authors, including:

Yong Hou

National University of Defense Technology

23 PUBLICATIONS **148** CITATIONS

SEE PROFILE

Jiayu Dai

National University of Defense Technology

31 PUBLICATIONS **555** CITATIONS

SEE PROFILE

Dongdong Kang

National University of Defense Technology

13 PUBLICATIONS **119** CITATIONS

SEE PROFILE

Jianmin Yuan

National University of Defense Technology

233 PUBLICATIONS **1,858** CITATIONS

SEE PROFILE

Equations of state and transport properties of mixtures in the warm dense regime

Yong Hou, Jiayu Dai, Dongdong Kang, Wen Ma, and Jianmin Yuan

Citation: Physics of Plasmas (1994-present) **22**, 022711 (2015); doi: 10.1063/1.4913424
View online: http://dx.doi.org/10.1063/1.4913424
View Table of Contents: http://scitation.aip.org/content/aip/journal/pop/22/2?ver=pdfcov
Published by the AIP Publishing

Equations of state and transport properties of mixtures in the warm dense regime

Yong Hou,[1] Jiayu Dai,[1] Dongdong Kang,[1] Wen Ma,[1] and Jianmin Yuan[1,2,a)]
[1]*Department of Physics, College of Science, National University of Defense Technology, Changsha 410073, People's Republic of China*
[2]*IFSA Collaborative Innovation Center, Shanghai Jiao Tong University, Shanghai 200240, People's Republic of China*

(Received 9 March 2014; accepted 2 February 2015; published online 24 February 2015)

We have performed average-atom molecular dynamics to simulate the CH and LiH mixtures in the warm dense regime, and obtained equations of state and the ionic transport properties. The electronic structures are calculated by using the modified average-atom model, which have included the broadening of energy levels, and the ion-ion pair potentials of mixtures are constructed based on the temperature-dependent density functional theory. The ionic transport properties, such as ionic diffusion and shear viscosity, are obtained through the ionic velocity correlation functions. The equations of state and transport properties for carbon, hydrogen and lithium, hydrogen mixtures in a wide region of density and temperature are calculated. Through our computing the average ionization degree, average ion-sphere diameter and transition properties in the mixture, it is shown that transport properties depend not only on the ionic mass but also on the average ionization degree. © *2015 AIP Publishing LLC*. [http://dx.doi.org/10.1063/1.4913424]

I. INTRODUCTION

Warm dense matter (WDM)[1] regime includes the temperatures from a few electron-volt (eV) to a few hundreds and densities from a few hundredths to hundreds of the times of solid density. In this regime, the electrons are ionized with increasing temperature and localized with increasing density. Meanwhile, the ion-ion interactions should also be considered. The physical properties of WDM, such as the equation of state, radiative opacity[2] and the ionic structure, are important for the studies of astrophysics[3,4] and inertial confinement fusion (ICF).[5] These properties are the crucial input parameters in hydrodynamic simulations,[6,7] in particular, will affect the hydrodynamic instability in the process of the compression of ICF capsule. However, obtaining high temperature and density states required for experimental techniques is challenging; also it is difficult to describe the electronic and ionic structures simultaneously for theoretical calculations because all physical ingredients, such as coulomb interactions, bound-state level shifts, pressure ionization,[8,9] electron degeneracy and ion-ion strong coupling, must be taken into account. In particular, the physical properties of ions are affected by other ions in WDM regime, and these effects become more and more important with increasing density. Therefore, many models are proposed to describe electronic and ionic structures in this regime.

The one-component plasma (OCP) and the Yukawa model[10] combined with the Monte Carlo (MC) or molecular dynamics (MD) have been used to predict the ionic structures at high temperature and density. The results of these methods depend on one or two parameters, but the electron quantum effects are not included. Quantum molecular dynamics (QMD)[11–14] simulations, which treat the nuclei classically and the electrons quantum-mechanically by using the density functional theory (DFT), have proved to be appropriate for describing the transport property[7,15–18] and equation of state,[19–22] but these methods are computationally expensive, particularly at high temperature. The path integral Monte Carlo method[23–26] and molecular dynamics[27–29] can also give an appropriate description of the properties in the warm dense regime, however, the method is also computationally expensive and applied only to low-Z elements such as H, He, C, and H_2O (Ref. 26) so far. Thus, first principles methods are difficult to construct large data tables of material properties. Orbital-free molecular dynamics (OFMD),[30–32] in which electronic free energy is a local functional of the electronic density, can be used at high temperature. However, at present, OFMD is usually limited to a few hundred atoms. In our previous work,[15] we have discussed the relation between the number of ions and the transport properties of Fe. It was shown that the convergent results of the diffusion and viscosity coefficients need 4000 ions in performing molecular dynamics using the periodic boundary conditions. For the mixture, it is necessary to simulate a system with large number of ions. So we perform molecular dynamics to compute the transport properties including more ions for mixture.

In the present study, we investigate the equation of state and ionic transport properties of the mixtures through the average-atom molecular dynamics (AAMD) simulations. In order to consider the electronic quantum effect, the electronic structures are obtained by solving the modified average-atom (AA) model,[33,34] which includes the thermal electron excitation and ionization in a statistical way.[35–37] The ionic pair potentials are obtained from the electronic densities overlap of two isolated ions based on the modified Gordon and Kim (GK)[38] theory in the framework of

a)Author to whom correspondence should be addressed. Electronic mail: jmyuan@nudt.edu.cn

temperature-depended density functional theory (td-DFT). When the interacting ions come together, the rearrangement of the nonlocal electrons is considered by retaining the total nonlocal charges of the interacting system unchanged. And the results obtained from the theory have been found to give excellent agreement with the known equations of state and ionic structures for Al and Fe.[39] In this work, we first present brief descriptions of the AAMD method and how to obtain dynamical properties, such as ionic diffusion and shear viscosity, in the WDM regime. Since the C, H mixture is major components of ablator and Li, H mixture is a possible alternative ablator for ICF, in Sec. III we apply the AAMD method to simulate the mixtures of CH and LiH, and calculate the equations of state and transport coefficients in the WDM regime. And in Sec. IV, we give the summary.

II. METHODS OF CALCULATION

In this section, we first give brief descriptions about how to set up the model and to obtain ionic pair potential of mixtures in the WDM regime. And then we discuss the implementation of various schemes to determine the dynamical properties, such as ionic diffusion and shear viscosity.

A. AAMD method

For an isolated ion, the electronic density distribution is calculated by the modified AA model,[33,34] which considers the electronic energy level broadening and includes the temperature and density effects on the electronic distributions in a statistical way. Each ion is described as an ion-sphere, in which the electronic density of bound state (eigenvalue $E<0$) is obtained by solving the Dirac equation and free electronic ($E>0$) density from the Thomas-Fermi (TF) approximation. When we calculate the pair-potential, the total electronic density is divided into two parts: the uniformly nonlocal distributed free-electron sea $\rho(r_b)$ in the whole space which is equal to the density of electrons at the ion-sphere boundary, r_b, and the local electrons $\rho_i^{2nd}(r)$ equal to the total electron density minus the first constant distribution, representing the dramatic space variation of the electronic distribution around the nucleus. The atomic volume is proportional to the nuclear charge and the sum of the local electrons within each atomic sphere. Because the integration of the local electron density within an atomic sphere needs the atomic size in advance, the calculation is carried out in a self-consistent way for the isolated atoms. When we calculate ion-ion pair potentials, the spatial distribution of the nonlocal free electrons changes with two ions coming closer, but the density remains unchanged, see Fig. 1 of Ref. 39. The localized electrons will overlap each other, and the total density of the local electrons is the sum of the two separate ions in the overlap region. In order to keep the electronic density of the nonlocal free-electron sea unchanged, when the electrons of two ions become overlapped, the boundary changes in such a way that the truncated spherical volume equal to the sum of the two separated ions to keep the electrical neutrality in the whole interaction region.[39] Thus, the total density is $\rho = \rho_A^{2nd} + \rho_B^{2nd} + \rho(r_b)$, where A and B represent different ions, respectively.

The pair potentials are computed through

$$V(R) = V_{Coul}(R) + V_k(R) + V_e(R) + V_c(R), \tag{1}$$

where R is the distance between two nuclei, $V_{Coul}(R)$ is the static Coulomb energy, $V_k(R)$ is the kinetic energy, $V_e(R)$ and $V_c(R)$ are the exchange and correlation energies, respectively. $V_{Coul}(R)$ can be calculated directly from the electronic density based on the GK theory.[38] The last three terms in Eq. (1) can be, respectively, calculated through integral of the kinetic energy $E_k(\rho)$, exchange energy $E_e(\rho)$ and correlation energy $E_c(\rho)$[38,40–42] in the spheroidal coordinate system, $\lambda_1 = (r_1 + r_2)/R, \lambda_2 = (r_1 - r_2)/R$, using the Gauss-Legendre numerical quadrature,

$$V_k(R) = \pi \int\int d\lambda_1 d\lambda_2 \cdot r_1 \cdot r_2 \times \{\rho E_k(\rho) - \rho_A E_k(\rho_A) - \rho_B E_k(\rho_B)\}, \tag{2}$$

$$V_e(R) = \pi \int\int d\lambda_1 d\lambda_2 \cdot r_1 \cdot r_2 \times \{\rho \cdot E_e(\rho) - \rho_A E_e(\rho_A) - \rho_B E_e(\rho_B)\}, \tag{3}$$

$$V_c(R) = \pi \int\int d\lambda_1 d\lambda_2 \cdot r_1 \cdot r_2 \times \{\rho \cdot E_c(\rho) - \rho_A E_c(\rho_A) - \rho_B E_c(\rho_B)\}. \tag{4}$$

And when calculating $E_k(\rho)$, $E_e(\rho)$, and $E_c(\rho)$, we consider the effect of the temperature. The energies are expressed as

$$E_k(\rho) = \frac{\sqrt{2}}{\pi^2 \rho} \int \frac{\epsilon^{3/2}}{\exp\big((\epsilon - \mu)/T\big) + 1} d\epsilon, \tag{5}$$

$$E_e(\rho) = -0.6109 r_s^{-1} \times \frac{1 + 2.83431t^2 - 0.21512t^3 + 5.27586t^4}{1 + 3.94309t^2 + 7.91379t^4} \times \tanh(t^{-1}), \tag{6}$$

$$E_c(\rho) = -0.6109 r_s^{-1/2} \times \frac{-0.0081 + 1.127t^2 + 3.756t^4}{1 + 1.291t^2 + 3.593t^4} \tanh(t^{-1/2}), \tag{7}$$

where the $r_s = 0.6203474\rho^{-1/3}$, and $t = 0.543 r_s T$, T is electronic temperature. The difference between the present model and the original GK theory is that the electronic density distribution of the isolated ion is divided into two parts, i.e., the electronic sea $\rho(r_b)$ and the local electron $\rho_i^{2nd}(r)$.

Molecular dynamics are performed in the cubic volume V to simulate the mixture based on the pair-potentials described above. The mixture ions are included to perform simulations with the NVT (constant N, number of particles; V, volume; and T, temperature) ensemble. The system is assumed to be in local thermodynamics equilibrium, and the electronic and ionic temperatures are considered to be equal. Each MD simulation consists of two stages: the equilibration stage and the production stage. At the production stage, the physical properties of the matter are obtained by averaging over the time. The results of MD

simulations in the NVT ensemble depend on the number of time steps n_t, size of the time step δt, number of ions N, and the cutoff r_{cutoff}. In order to obtain accurate results, we simulate the time steps $n_t = 100\,000$ for all the results, where first $n_t = 10\,000$ time steps are used to arrive at equilibration and another time steps are applied to calculate the correlation function. And r_{cutoff} is the sum of the two ionic radius, which are determined by the ion number density n_i and the average ionization degree in the self-consistent way. The time step δt of the MD simulation is determined by the plasma temperature and density, $\delta t \sim r_{ws}/T^{1/2}$, where r_{ws} is the Wigner-Seitz radius. And the Wigner-Seitz radius of each ion depends on the ionic number density and average ionization degree.[37] When we use the r_{ws} to calculate the time step, the smaller one is chosen for mixture. The initial configuration of the ion is set as the ideal fcc crystal structure.

B. Ion transport properties

Based on molecular dynamics simulations, we calculate the ionic diffusion and shear viscosity coefficient. The self-diffusion coefficient is calculated by the velocity autocorrelation function[43]

$$D_\alpha = \frac{1}{3}\int \langle v_i(t) v_i(0)\rangle dt, \tag{8}$$

where the v_i is the ith ionic velocity of the species α. The mutual diffusion coefficient is obtained from the autocorrelation function

$$D_{\alpha\beta} = \frac{1}{3Nx_\alpha x_\beta}\int \langle A(t)A(0)\rangle dt \tag{9}$$

with

$$A(t) = x_\beta \sum_{i=1}^{N_\alpha} v_i(t) - x_\alpha \sum_{j=1}^{N_\beta} v_j(t), \tag{10}$$

where $x_{\alpha,\beta} = N_{\alpha,\beta}/N$. $N = N_\alpha + N_\beta$ represents the number of ions, $N_{\alpha,\beta}$ is the number of the species α or β in the mixture. The mutual diffusion coefficient can also be calculated from the self-diffusion coefficient if the inter-species interactions are smaller than the intra-species interactions[32]

$$D_{\alpha\beta} = x_\beta D_\alpha + x_\alpha D_\beta. \tag{11}$$

The viscosity coefficient is calculated from the autocorrelation function of the off-diagonal component of the stress tensor

$$\eta = \frac{V}{k_B T}\int_0^t \langle P_{12}(0) P_{12}(t')\rangle dt', \tag{12}$$

where k_B is the Boltzmann's constant, P_{12} represents the five independent off-diagonal component of stress tensor P_{xy}, P_{yz}, P_{zx}, $(P_{xx} - P_{yy})/2$, $(P_{yy} - P_{zz})/2$, respectively.

III. RESULT AND DISCUSSION

Based on the method described above, we performed the AAMD to calculate equations of state and the transport properties of the CH and LiH mixtures in the warm dense regime. 13 500 atoms are initially arranged into the ideal fcc crystal structure with the lattice constant corresponding to the given density.

First, we calculate the pressures of the C_2H_3 mixture with increasing temperature at the densities of 7 g/cm^3 and 9 g/cm^3, as shown in Fig. 1, including both the ionic and electronic contributions. The ionic pressures are extracted from the MD simulations by using the classical virial expressions: $PV = NK_BT + \frac{1}{3} < \sum_i x_i \frac{\partial U}{\partial x_i} >$ as in Ref. 39; The electronic pressures of the mixture are calculated from the modified AA model[33,34] and depend on the electronic density of the ionic boundary, which is contributed largely from the free electrons. In Fig. 1, comparisons are made with the results of QEOS, QMD, and OFMD.[31] QEOS represents the quotidian equation of state model[44] where ionic contributions are calculated from the Yukawa model.[45] At the density of 9 g/cm^3, the AAMD's results agree with the other results very well, except for the points at the temperature of 5 eV. We also see that the AAMD's and OFMD's results are in good agreement over the temperature range considered here. This is due to the fact that both the AAMD's and OFMD's electronic pressures are calculated with Thomas-Fermi (TF) approximation and the ionic pressure contribution to the total pressure is smaller in this regime. In the calculations of ionic pressures, we only consider the ionic pair-potentials in the AAMD method, neglecting many-body effects. At lower temperature, the difference between the OFMD's and QMD's results appears. The electronic energy levels have been broadened and become the energy bands with decreasing temperature. So the difference between the AAMD, OFMD, and QMD becomes apparent at low temperature.

The comparisons of ionic diffusion coefficients between the results of AAMD and OFMD[31] are shown in Figs. 2 and 3 for the mixture of C_2H_3 at the densities of 7 g/cm^3 and 9 g/cm^3,

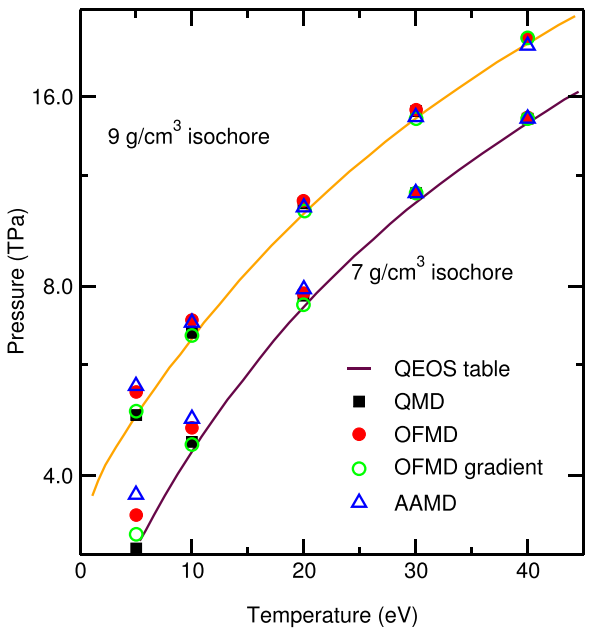

FIG. 1. Pressure versus temperature for C_2H_3 mixture along the two isochores, 7 g/cm^3 and 9 g/cm^3 calculated by different methods: QMD (square), OFMD (circle), AAMD (triangle), and QEOS (line) table.

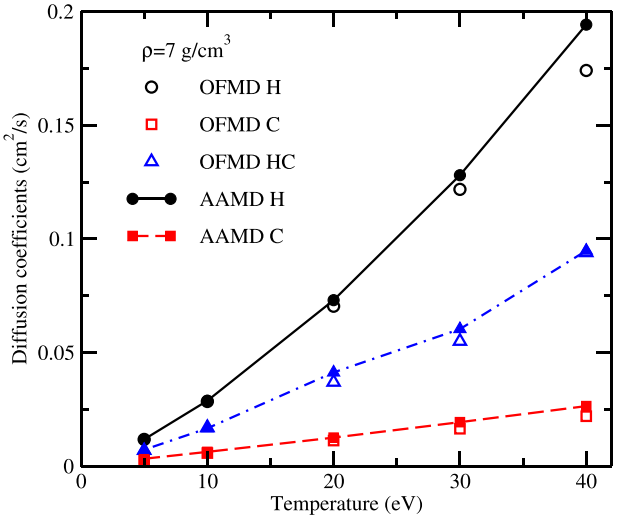

FIG. 2. The self- and mutual diffusion coefficients for C_2H_3 mixture using the OFMD and AAMD methods as a function of temperature at the density of 7 g/cm^3. The self-diffusion coefficients for C are labeled by squares, and that for H labeled by circles, and triangles up represent the mutual diffusion coefficients.

respectively. The two figures give the self-diffusion coefficients of H, C, and mutual diffusion coefficients of HC with increasing temperature. These diffusion coefficients are obtained through velocity correlation functions. As shown in Figs. 2 and 3, mutual diffusion coefficients are in good agreement with the results of OFMD model. However, with increasing temperature, the difference of the self-diffusion coefficient between two models is shown. In our calculations, the AAMD method only considers the ionic pair-potentials, and OFMD considers the multi-ion interactions. At high density and low temperature, the ions vibrate only near the equilibrium positions, and each ion is trapped for some period of time in the cage formed by its immediate neighbors.[46] So ionic velocity is very small and ion interacts with the nearest-neighbor ion in some period of time, the two-body collision is enough to describe the ionic transport characters, which is different from the effect on equations of state. When the matter is in the solid state, the diffusion coefficients depend on the crystal lattice.[15] And with increasing temperature, the ions move in wide range in one time period, many-body correlation effects become important. So the difference between the two models becomes more obvious, such as the points whose temperature is higher above 20 eV. However, if the temperature continues increasing, the many-body correlation effect on the velocity correlation function becomes less, and the pair-ion correlation effects become dominated at higher temperature.[46] Fig. 4 shows the shear viscosity of the C_2H_3 mixture as a function of temperature at the densities of 7 g/cm^3 and 9 g/cm^3, respectively. The results are compared with those of OFMD[31] and OCP[47] methods. For the shear viscosity, it is similar to the diffusion. This is related to the ionic collision cross section. At low temperature, our results are in agreement with those of OFMD. With increasing temperature, the difference of two results becomes clear. However, for all the regime, there is a big difference between OCP's results and AAMD's results.

In order to explain the relations between transport property and collision cross section, we also calculate the ionic transport properties for LiH mixture at the temperature of 50 eV with different densities. In Fig. 5, The self- and mutual diffusion coefficients for the LiH mixture at the temperature of 50 eV and densities from ρ_0 ($=0.788$ g/cm^3) to $10 \times \rho_0$ are given using the AAMD and OFMD[32] methods. In Fig. 5, mutual diffusion coefficients calculated from the self-diffusion coefficients according to Eq. (11) are also shown. From the figure, we can see that at low and high densities the AAMD's results are in good agreement with those of OFMD for the self-diffusion coefficients of H and Li. However, our results are different from the OFMD's results at the densities of $3 \times \rho_0, 4 \times \rho_0$, and $5 \times \rho_0$. At the density of $10 \times \rho_0$, the state of plasma is similar to that at low temperature, in which each ion is trapped for some period of time in the cage and

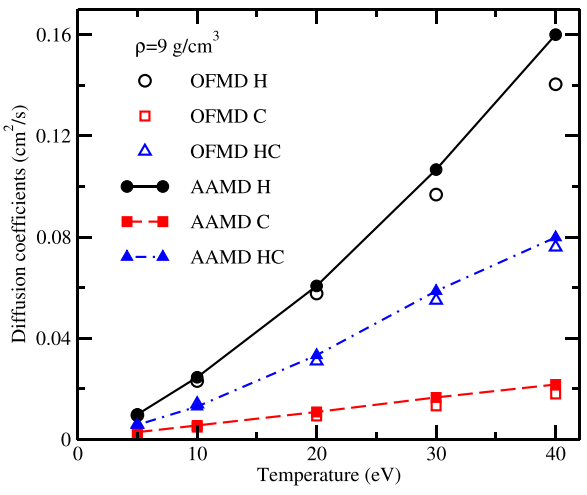

FIG. 3. The self- and mutual diffusion coefficients for C_2H_3 mixture using the OFMD and AAMD methods as a function of temperature at the density of 9 g/cm^3. The self-diffusion coefficients for C are labeled by squares, and that for H labeled by circles, and triangles up represent the mutual diffusion coefficients.

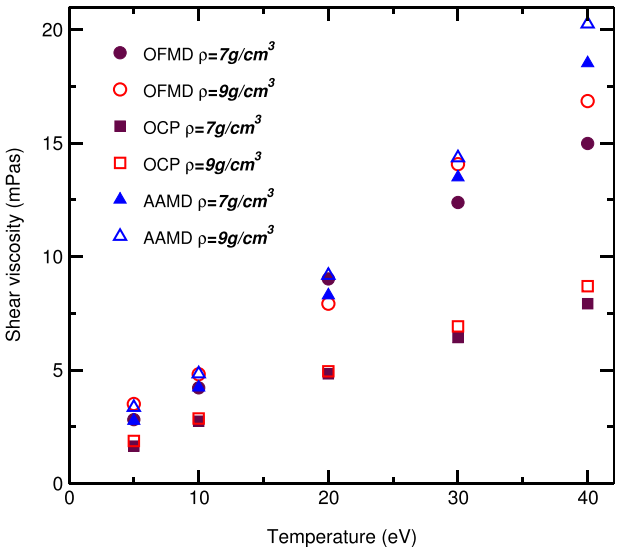

FIG. 4. The shear viscosity for C_2H_3 mixture using the OFMD, OCP,[31] and AAMD methods as a function of temperature at the densities of 7 g/cm^3 and 9 g/cm^3.

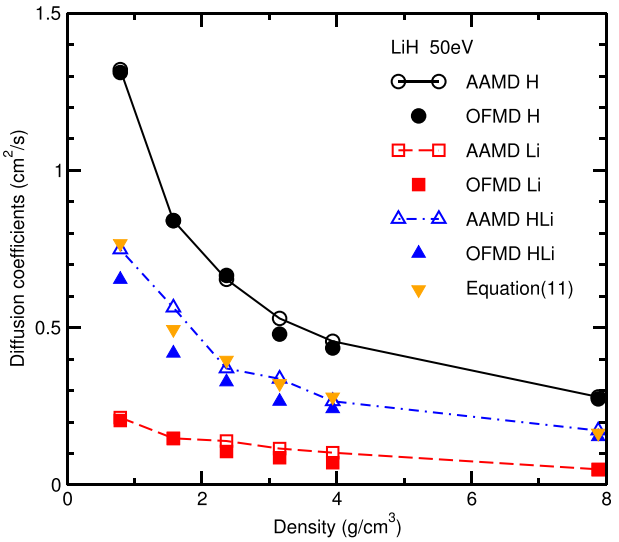

FIG. 5. The self- and mutual diffusion coefficients for LiH mixture using the OFMD and AAMD methods as a function of density at the temperature of 50 eV. Triangles down represent the date calculated from the self-diffusion coefficients C and H with Eq. (11).

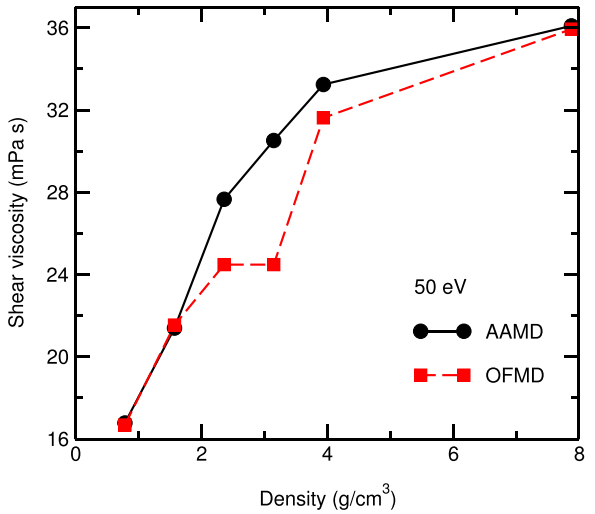

FIG. 6. The shear viscosity for LiH mixture using the OFMD[32] and AAMD methods as a function of density at the temperature of 50 eV.

only interacts with the nearest-neighbor ion. With decreasing density, the average distance between ions become larger and each ion collides with others more than one times in a period of time. So many-body interactions become important when calculating the diffusion coefficient in this regime. When the density reduces to the $2 \times \rho_0$, the average ionic distance will become very large and the many-body correlation effects contribution to the velocity correlation function are very small at the temperature of 50 eV, pair correlation effects become important. At the densities of $2 \times \rho_0$ and $1 \times \rho_0$, the AAMD's results are consistent with those of OFMD. And we calculate the mutual diffusion coefficients from the correlation function according to the Eq. (9) (labeled by triangle up points and dot-dashed line) and from the self-diffusion coefficients of H and Li according to the Eq. (11) (labeled by triangle down points). From the figure, we can see that the differences between the two results are very small. Therefore, it is shown that the inter-species interactions are smaller than the intra-species interactions. So in this regime, we can obtain the mutual diffusion coefficients from the self-diffusion coefficients and avoid the statistical error calculated from the velocity correlation functions.

In Fig. 6, we present the shear viscosities for the LiH mixture at the temperature of 50 eV and densities from ρ_0 ($=0.788\,\mathrm{g/cm^3}$) to $10 \times \rho_0$ comparing with the results of OFMD.[32] With increasing density, the interactions among different ions become stronger and the viscosities increase. Similar to the diffusion coefficients, there are big differences between the AAMD's and OFMD's results at the densities $3 \times \rho_0, 4 \times \rho_0$, and $5 \times \rho_0$. Besides the interaction of ions, the differences come from the different method of describing the electronic structure. OFMD method computes the electronic structures using the TF approximation, AAMD method describes the free electron by the TF approximation and the bound electron by the Dirac equation. So the two different descriptions of the electronic structure give the different average ionization degree, which has discussed in the Ref. 37 for the mixtures. In the Fig. 7, we give the average ionization degrees of Li and H in LiH mixture at the temperature of 50 eV. In order to show the results of H and Li in the same figure, the results of H have been plus 1. From the figure, we can see the shell structure effects, which the average ionization degrees of Li first decrease for the free electrons are pressured into the bound state and become the bound electrons and then increase due to the pressure ionization with increasing density. However, TF approximation does not consider the shell structure effects[37] and would give the different results of the average ionization degree when the effects are important. So the ionic interactions and collision cross sections are different using the two kinds of methods, and then transport properties will be different.

We calculate the ratio of the ion self-diffusion coefficient and the average ion-sphere diameter square between H and Li as a function of the density at the temperature of 50 eV for the mixture of LiH, as shown in Fig. 8. The average ion-sphere diameter is calculated from the modified average-atom model,[33,34] which is determined by the ion number density n_i and the average ionization degree in a self-consistent way. Due to the average ionization degrees of

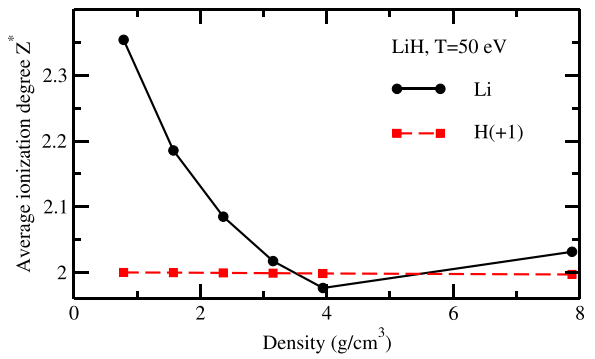

FIG. 7. The average ionization degree of Li and H in LiH mixture using modified AA method as a function of density at the temperature of 50 eV. Solid line with cycles is the results of Li and dashed line with squares is that of H. In order to show the results of H and Li in the same figure, the results of H have been plus 1.

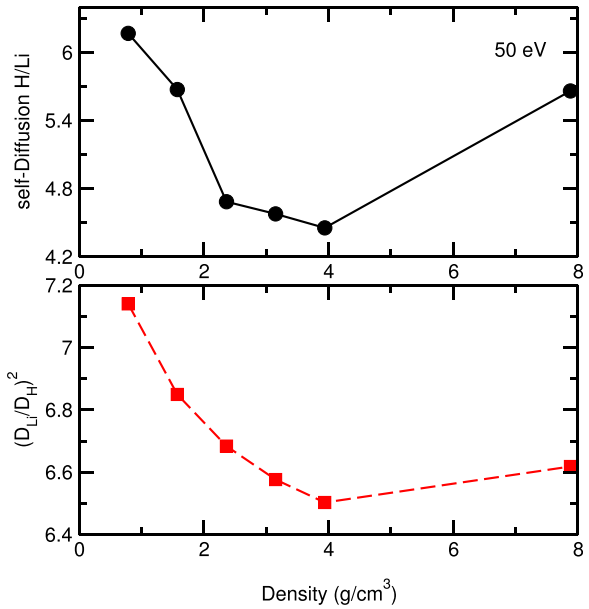

FIG. 8. The self-diffusion coefficient ratio of H/Li and the average ion-sphere diameter square ratio of Li/H as a function of density at the temperature of 50 eV.

H are almost equal to 1 in the regime, the trend of the ratio of average ion-sphere diameter square is very similar to that of the Li average ionization degree. From the figure, we can also see that the trend of two curves is very similar with increasing density. It is shown that the ionic diffusion coefficient is closely related to the average ion-sphere diameter square. When the density is very low, the self-diffusion coefficient of H is about six times higher than that of Li. This is because that the ion diffusions depend on the ionic mass primarily. With increasing density, the thermo-ionized electrons are pressed into the ion-sphere and the average ionization degrees of Li become smaller, so the average ion-sphere diameter becomes smaller relative to that of H. And the self-diffusion coefficient of Li will rise relative to that of H as shown in Fig. 8. However, when pressure ionization of Li happens at the $10 \times \rho_0$, the average ionization degree and the ion-sphere diameter of Li become larger relative to that of H, the self-diffusion coefficient of Li will reduce. Therefore, the ionic diffusion coefficient is dependent not only on the ionic mass but also on the ionic ionization degree.

IV. CONCLUSION

The equations of state and transport properties of the C_2H_3 and LiH mixtures are calculated using the AAMD method in the warm dense regime. Through comparisons with the OFMD method and other theoretical methods, it is shown that the AAMD methods can be used to describe the mixture properties in the warm dense regime except at very low temperature. In addition, through comparing the self-diffusion coefficient with the average ionization degree, we have showed that the transport properties depend not only on the ionic mass but also on the average ionic ionization degree. It can be explained that the ion charge will affect the ionic collision cross section and transport properties. However, the present molecular dynamic method only simulates the average ionic state. In the future, we will develop molecular dynamics including different ion-charge state to simulate the transport properties of the system with the different ion-charge states.

ACKNOWLEDGMENTS

This work was supported by the National Natural Science Foundation of China under Grant Nos. 11005153, 11274383, and 11422432. Funding support (SKLLIM1107) from state key laboratory of laser interaction with matter is acknowledged. We are grateful for the comments of the anonymous referees.

[1]R. W. Lee, H. A. Baldis, R. C. Cauble, O. L. Landen, J. S. Wark, A. Ng, S. J. Rose, C. Lewis, D. Riley, J.-C. Gauthier, and P. Audebert, Laser Part. Beams **20**, 527 (2002).
[2]J. Zeng and J. Yuan, Phys. Rev. E **66**, 016401 (2002); **74**, 025401(R) (2006).
[3]M. D. Knudson, M. P. Desjarlais, R. W. Lemke, T. R. Mattsson, M. French, N. Nettelmann, and R. Redmer, Phys. Rev. Lett. **108**, 091102 (2012).
[4]D. C. Swift, J. H. Eggert, D. G. Hicks, S. Hamel, K. Caspersen, E. Schwegler, G. W. Collins, N. Nettelmann, and G. J. Ackland, Astrophys. J. **744**, 59 (2012).
[5]B. Remington, R. P. Drake, and D. Ryutov, Rev. Mod. Phys. **78**, 755 (2006).
[6]J.-F. Danel, L. Kazandjian, and G. Zérah, Phys. Rev. E **85**, 066701 (2012).
[7]J. D. Kress, J. S. Cohen, D. A. Horner, F. Lambert, and L. A. Collins, Phys. Rev. E **82**, 036404 (2010).
[8]S. M. Vinko, S. M. Vinko, O. Ciricosta, B. I. Cho, K. Engelhorn, H.-K. Chung, C. R. D. Brown, T. Burian, J. Chalupsk, R. W. Falcone, C. Graves, V. Hjkov, A. Higginbotham, L. Juha, J. Krzywinski, H. J. Lee, M. Messerschmidt, C. D. Murphy, Y. Ping, A. Scherz, W. Schlotter, S. Toleikis, J. J. Turner, L. Vysin, T. Wang, B. Wu, U. Zastrau, D. Zhu, R. W. Lee, P. A. Heimann, B. Nagler, and J. S. Wark, Nature **482**, 59 (2012).
[9]T. R. Preston, S. M. Vinko, O. Ciricosta, H.-K. Chung, R. W. Lee, and J. S. Wark, High Energy Density Phys. **9**, 258 (2013).
[10]J. P. Hansen and I. R. McDonald, *Theory of Simple Liquids* (Academic Press, London, 1990).
[11]M. P. Desjarlais, Phys. Rev. B **68**, 064204 (2003).
[12]F. R. Krajewski and M. Parrinello, Phys. Rev. B **73**, 041105(R) (2006).
[13]T. D. Kuhne, M. Krack, F. R. Mohamed, and M. Parrinello, Phys. Rev. Lett. **98**, 066401 (2007).
[14]S. Mazevet, F. Lambert, F. Bottin, G. Zérah, and J. Clérouin, Phys. Rev. E **75**, 056404 (2007).
[15]J. Dai, Y. Hou, D. Kang, H. Sun, J. Wu, and J. Yuan, New J. Phys. **15**, 45003 (2013).
[16]D. A. Horner, F. Lambert, J. D. Kress, and L. A. Collins, Phys. Rev. B **80**, 024305 (2009).
[17]C. Wang, X.-T. He, and P. Zhang, Phys. Rev. E **88**, 033106 (2013); C. Wang, Y. Long, X.-T. He, J.-F. Wu, W.-H. Ye, and P. Zhang, *ibid.* **88**, 013106 (2013).
[18]S. X. Hu, L. A. Collins, T. R. Boehly, J. D. Kress, V. N. Goncharov, and S. Skupsky, Phys. Rev. E **89**, 043105 (2014).
[19]J. Dai, Y. Hou, and J. Yuan, Phys. Rev. Lett. **104**, 245001 (2010); Astrophys. J. **721**, 1158 (2010); J. Dai, D. Kang, Z. Zhao, Y. Wu, and J. Yuan, Phys. Rev. Lett. **109**, 175701 (2012).
[20]C. Wang, X.-T. He, and P. Zhang, Phys. Plasmas **18**, 082707 (2011).
[21]S. Hamel, L. X. Benedict, P. M. Celliers, M. A. Barrios, T. R. Boehly, G. W. Collins, T. Döppner, J. H. Eggert, D. R. Farley, D. G. Hicks, J. L. Kline, A. Lazicki, S. Lepape, A. J. Mackinnon, J. D. Moody, H. F. Robey, E. Schwegler, and P. A. Sterne, Phys. Rev. B **86**, 094113 (2012).
[22]S. X. Hu, T. R. Boehly, and L. A. Collins, Phys. Rev. E **89**, 063104 (2014).
[23]W. R. Magro, D. M. Ceperley, C. Pierleoni, and B. Bernu, Phys. Rev. Lett. **76**, 1240 (1996).
[24]B. Militzer and D. M. Ceperley, Phys. Rev. Lett. **85**, 1890 (2000).
[25]A. V. Filinov, M. Bonitz, and Yu. E. Lozovik, Phys. Rev. Lett. **86**, 3851 (2001).

[26]K. P. Driver and B. Militzer, Phys. Rev. Lett. **108**, 115502 (2012).
[27]M. A. Morales, J. M. McMahon, C. Pierleoni, and D. M. Ceperley, Phys. Rev. Lett. **110**, 065702 (2013).
[28]D. Kang, J. Dai, H. Sun, Y. Hou, and J. Yuan, Sci. Rep. **3**, 3272 (2013).
[29]D. Kang, H. Sun, J. Dai, W. Chen, Z. Zhao, Y. Hou, J. Zeng, and J. Yuan, Sci. Rep. **4**, 5484 (2014).
[30]F. Lambert, J. Clérouin, and G. Zérah, Phys. Rev. E **73**, 016403 (2006); F. Lambert, J. Clérouin, J.-F. Danel, L. Kazandjian, and G. Zérah, *ibid.* **77**, 026402 (2008).
[31]F. Lambert and V. Recoules, Phys. Rev. E **86**, 026405 (2012).
[32]L. Burakovsky, C. Ticknor, J. D. Kress, L. A. Collins, and F. Lambert, Phys. Rev. E **87**, 023104 (2013).
[33]Y. Hou, F. Jin, and J. Yuan, Phys. Plasma **13**, 093301 (2006).
[34]Y. Hou, F. Jin, and J. Yuan, J. Phys.: Condens. Matter **19**, 425204 (2007).
[35]B. F. Rozsnyai, Phys. Rev. A **5**, 1137 (1972); D. A. Liberman, Phys. Rev. B **20**, 4981 (1979).
[36]G. Faussurier, C. Blancard, and A. Decoster, Phys. Rev. E **56**, 3474 (1997); **56**, 3488 (1997).
[37]J. Yuan, Phys. Rev. E **66**, 047401 (2002).
[38]R. G. Gordon and Y. S. Kim, J. Chem. Phys. **56**, 3122 (1972); Y. S. Kim and R. G. Gordon, Phys. Rev. B **9**, 3548 (1974).
[39]Y. Hou and J. Yuan, Phys. Rev. E **79**, 016402 (2009).
[40]J. C. Slater, *Quantum Theory of Atomic Structure* (Mcgraw-Hill, 1960), Vol. 2.
[41]W. J. Carr, R. A. Coldwell-Horsfall, and A. E. Fein, Phys. Rev. **124**, 747 (1961); W. J. Carr and A. A. Maradudin, Phys. Rev. **133**, A371 (1964).
[42]J. Yuan, Y. Zhao, and Z. Zhang, Acta Mech. Sin. **21**(4), 479 (1989) (in Chinese).
[43]M. P. Allen and D. J. Tildesley, *Computer Simulation of Liquids* (Clarendon Press, Oxford, 1987).
[44]R. M. More, K. H. Warren, D. A. Young, and G. B. Zimmerman, Phys. Fluids **31**, 3059 (1988).
[45]D. Gilles, F. Lambert, J. Clérouin, and G. Salin, High Energy Density Phys. **3**, 95 (2007).
[46]J. Daligault, Phys. Rev. Lett. **96**, 065003 (2006).
[47]S. Bastea, Phys. Rev. E **71**, 056405 (2005).